J Antimicrob Chemother 2012; **67**: 2650–2660
doi:10.1093/jac/dks286 Advance Access publication 7 August 2012

Journal of Antimicrobial Chemotherapy

Development of nanocapsules bearing doxorubicin for macrophage targeting through the phosphatidylserine ligand: a system for intervention in visceral leishmaniasis

Shaswat Kansal[1], Rati Tandon[2], Pankaj Dwivedi[1], Pragya Misra[2], P. R. P. Verma[3], Anuradha Dube[2] and Prabhat Ranjan Mishra[1]*

[1]*Pharmaceutics Division, CSIR-Central Drug Research Institute, Chattar Manzil Palace, Lucknow 226001, India;* [2]*Parasitology Division, CSIR-Central Drug Research Institute, Lucknow 226001, India;* [3]*Department of Pharmaceutical Sciences, Birla Institute of Technology, Mesra, Ranchi 835215, India*

*Corresponding author. Tel: +0522-2612411-18; E-mail: mishrapr@hotmail.com

Received 20 March 2012; returned 4 May 2012; revised 14 June 2012; accepted 27 June 2012

Objectives: The purpose of this study was to explore the applicability, targeting potential and drug delivery to specialized phagocytes via phosphatidylserine (PS)-specific ligand-anchored nanocapsules (NCs) bearing doxorubicin.

Methods: The layer-by-layer method was utilized to prepare NCs having a nanoemulsion core loaded with doxorubicin (NCs-DOX), which was further grafted with PS. PS-coated NCs (PS-NCs-DOX) were compared with NCs-DOX for *in vitro* targeting ability by studying uptake by macrophages, intracellular localization, *in vivo* pharmacokinetics and organ distribution studies. The *in vivo* antileishmanial activity of free doxorubicin, NCs-DOX and PS-NCs-DOX was tested against visceral leishmaniasis in *Leishmania donovani*-infected hamsters.

Results: Flow cytometric data revealed 1.75-fold enhanced uptake of PS-NCs-DOX in J774A.1 macrophage cell lines compared with NCs-DOX. *In vivo* organ distribution studies in Wistar rats demonstrated a significantly higher extent of accumulation of PS-NCs-DOX compared with NCs-DOX in macrophage-rich organs, particularly in liver and spleen. Highly significant antileishmanial activity ($P<0.05$ compared with NCs) was observed with PS-NCs-DOX, causing $85.23\% \pm 4.49\%$ inhibition of splenic parasitic burden. NCs-DOX and free doxorubicin caused only $72.88\% \pm 3.87\%$ and $42.85\% \pm 2.11\%$ parasite inhibition, respectively, in *Leishmania*-infected hamsters ($P<0.01$ for PS-NCs-DOX versus free doxorubicin and NCs-DOX versus free doxorubicin).

Conclusions: We conclude that the PS targeting moiety can provide a new insight for efficient drug delivery to specialized macrophages and thus may be developed for effective use in macrophage-specific delivery systems, especially for leishmaniasis.

Keywords: layer-by-layer assembly, polyelectrolytes, J774A.1 cell lines, *L. donovani*, amastigotes

Introduction

Leishmaniasis is a worldwide public health problem and is caused by various species of the genus *Leishmania* and is mainly associated with cutaneous, mucosal and visceral infections. It is characterized by fever and inflammation in the spleen and liver in humans.[1,2] The disease is also associated with several pathophysiological lethal-cascading events without specific chemotherapy. Visceral leishmaniasis is caused by *Leishmania donovani*, which resides and multiplies within macrophages of the mononuclear phagocytic system (MPS). The MPS is of emerging importance both scientifically and therapeutically because of its crucial role in inflammation. For many diseases, such as asthma, atherosclerosis and cancer, and for pathogenic infections, including tuberculosis, filariasis and leishmaniasis, the inflammatory process is a key driver of both disease progression and pathogenesis.[3–5] Therefore, the development of delivery systems that can target monocytes/macrophages intracellularly is crucial and could potentially open up new treatment paradigms for a range of diseases.

Macrophages express various engulfment receptors that are able to bind modified lipoproteins, senescent and apoptotic cells, proteins, polysaccharides and a range of polyanionic molecules.[6] The clearance of apoptotic cells by macrophages is an

integral component of normal life. Several researchers have reported that phosphatidylserine (PS) is exposed on the outer surface of apoptotic cells and that recognition of PS is important for the resulting anti-inflammatory responses that are induced by macrophages.[7] PS is a key ligand and is thought to exist in patches on apoptotic cells.

Recognition of PS involves multiple receptors, including some that can recognize naked PS and function together with other receptors that bind bridging protein bound to PS.[8] Several receptors have been suggested to play a crucial role in mediating PS recognition, including scavenger receptors, CD68 [an oxidized low-density lipoprotein (oxLDL) receptor], CD14, annexins, β2 glycoprotein I and GAS6.[9] Several groups of investigators have found that human and rodent macrophages, as well as insect phagocytes, preferentially take up negatively charged liposomes, particularly those containing PS.[10,11] Currently available chemotherapeutic agents for leishmaniasis show potential toxicity and serious adverse effects, which ultimately lead to narrow therapeutic applications. Earlier antimonials were regarded as first-line therapy for leishmaniasis, but various pieces of evidence show resistance of *Leishmania* amastigotes to the antimonials.[12] Doxorubicin, an anthracycline antibiotic used for the chemotherapy of various human cancers, was found to have potential antileishmanial activity, but its associated cardiac toxicity limits its clinical use.[13–15] Aspects of the toxicity related to the delivery of doxorubicin can be reduced by its specific delivery to intracellular regions of macrophages. Various researchers have reported that incorporation of doxorubicin in liposomes[16] and layer-by-layer (LBL)-assembled microcapsules[17] can increase the therapeutic index by reducing cardiotoxicity.

The above perspectives led us to explore the applicability, targeting potential and drug delivery to the macrophages via PS-specific ligand-anchored nanocapsules (NCs) bearing doxorubicin. We have developed NCs based on LBL technology having a nanoemulsion as a core, in which doxorubicin is loaded. The nanoemulsion was chosen as a core to improve the loading efficiency of doxorubicin, since free doxorubicin base has higher affinity for the internal oil phase, which restricts its entry into the external aqueous phase.[18] Moreover, doxorubicin imposes steric hindrance, resulting in low entrapment in structured vehicles such as liposomes.

The PS moiety provides an alternative means of targeting macrophages, and can easily be coated on cationic NCs due to its strongly anionic nature. Thus, in the present study we prepared and characterized PS-coated NCs loaded with doxorubicin (PS-NCs-DOX) and compared them with non-PS-coated NCs loaded with doxorubicin (NCs-DOX) for potential ability to target *L. donovani* parasites. Enhanced uptake can lead to smaller doses that are adequate for optimal therapeutic effect, thereby reducing the toxicity of the medication and providing a more efficient drug delivery system. PS-NCs-DOX are a candidate for macrophage-targeted drug delivery that can bind to macrophages in the liver and spleen and target the bioactive molecule inside them.

Materials and methods

Materials

PS (1,2-diacyl-*sn*-glycero-3-phospho-L-serine), sodium alginate (SA), protamine sulphate (PRM) and poly(sodium 4-styrenesulphonate) (PSS), mol. wt 70000, were purchased from Sigma-Aldrich, USA. Tween 80 and Span 80 were obtained from HiMedia Laboratories Pvt Ltd, Mumbai, India. Soyabean oil (SBO) was purchased from Sunshine Oleochem Ltd, Gandhidham, India. Dialysis membrane (mol. wt cut-off 70 kDa) was obtained from Sigma-Aldrich, USA. The annexin V-FITC apoptosis detection kit was obtained from Calbiochem, CA, USA. For cell culture, Dulbecco's modified Eagle's medium (DMEM) with glutamate, fetal bovine serum (FBS) and antibiotic solution (penicillin/streptomycin, 0.1% v/v) were purchased from Sigma-Aldrich, USA. MTT was also purchased from Sigma-Aldrich, USA. Well plates for cytotoxicity and uptake studies were from Greiner Bio One (Frickenhausen, Germany). All materials were used without further purification. The water used in all experiments was prepared in a three-stage Millipore Milli-Q Plus 185 purification system (Bedford, MA, USA) and had a resistivity >18.2 mW/cm. All polyelectrolytes were used without further purification. All other chemicals and solvents were of analytical grade.

Preparation of NCs containing nanoemulsion core

The emulsion inversion point method, a low-energy emulsification method,[19] was used to obtain a nanoemulsion core. It was obtained from a mixture of SBO (20 wt%) containing free doxorubicin base and weight ratio of Span 80/Tween 80 of ∼0.43/0.57 by slowly adding aqueous phase containing PSS (0.025 wt%) at a rate of 1.0 mL/min with gentle agitation using a magnetic stirrer at a temperature of 60°C. Free doxorubicin base was obtained using triethylamine-doxorubicin at a molar ratio of 3.[20] Ten millilitres of an aqueous polyelectrolyte solution of PRM (0.125%, w/v) was injected into the pre-formed nanoemulsion core. Adsorption of the polyelectrolyte was allowed for 45 min, during which time the dispersion was occasionally stirred. The procedure was repeated to coat oppositely charged SA (0.150%, w/v). Then, the dispersion was centrifuged for 15 min at 4000 rpm to separate the NCs from un-utilized polyelectrolye aggregates. Finally, the layer of PRM was assembled on the SA layer.

Coating of NCs with PS

Coating of NCs with PS was initiated as described elsewhere with slight modification.[21] Initially, PS was dissolved in chloroform:methanol (19:1) and evaporated in a rotary evaporator at 50°C and then hydrated with an aqueous dispersion of NCs for 20 min. The sample was then centrifuged at 40000 rpm for 30 min, after which the aqueous phase (lower layer) was withdrawn precisely to remove remaining lipid from the bulk. The PRM/PS weight ratio (process variable) was optimized by measuring the change in zeta-potential of the dispersion in triple-distilled water at 25°C (Zetasizer 3000 HS; Malvern Instruments Co., UK).

Characterization of NCs

Developed formulations were characterized prior to and after surface ligand anchoring. For morphological characterization, transmission electron microscopy (TEM; 400T TEM, Philips, New Brunswick, Canada) studies were carried out using phosphotungstic acid as a negative stain. TEM was carried out to determine the surface characteristics of the optimized formulations in aqueous medium using a 3 mM forman (0.5% plastic powder in amyl acetate)-coated copper grid (300 mesh) at 60 kV using negative staining by 2% phosphotungstic acid at various magnifications. The presence of PS on the surface of NCs was verified by determining the change in zeta-potential and measuring the characteristic fluorescence of an FITC-conjugated PS-specific protein, annexin V, using a Cary Eclipse Fluorescence Spectrophotometer (Agilent Technologies, USA). Differential scanning calorimetry (DSC) was performed with a Diamond DSC (PerkinElmer, USA) to exclude the formation of PS vesicles during coating. Control measurement was performed by using a pure

dispersion of PS vesicles with a concentration of 1 mg/mL. The mean particle size and size distribution of NCs and PS-NCs were determined using a Zetasizer Nano-ZS (Malvern Instruments). The NC dispersion was centrifuged at 40000 rpm for 20 min. The NCs were then separated and the amount of doxorubicin entrapped was determined by extracting the drug from the NCs using methylene chloride and analysed using reverse-phase HPLC.[22]

Macrophage uptake studies

The adherent mouse macrophage cell line J774A.1 was used for the present study, using a fluorescence-activated cell sorter (FACS; FACSAria, BD Biosciences, Germany). Aliquots (100 μL) containing J774A.1 (1×10^5) cells were suspended in 0.9 mL of fresh RPMI-1640 medium (Himedia) supplemented with 10 U/mL penicillin, 10% FBS, 100 μg/mL of streptomycin, 1 mM sodium pyruvate and 10 mM HEPES medium.[23] These were transferred into 24-well plates (Sigma, Germany) containing fresh medium and suspended in a 37°C humidified incubator with a 5% CO_2 atmosphere. After 24 h the culture medium was replaced with fresh culture medium containing NCs-DOX and PS-NCs-DOX formulations. To separate the internalized and surface-bound NCs, the cells were washed three times with acetate buffer (pH 4.0). The cell-associated fluorescence was measured by FACS at an excitation wavelength of 480 nm and an emission wavelength of 550 nm.[24] Macrophage uptake of PS-NCs-DOX was also assessed by confocal laser scanning microscopy (CLSM). Cells seeded at a density of 1×10^6 cells/well on poly-L-lysine-coated glass cover slips (in six-well plates) were left for 12 h, and then adherent macrophage monolayers were washed and incubated in fresh medium. PS-NCs-DOX were suspended in DMEM and added to macrophages and incubated for 4 h at room temperature in the dark. After incubation, monolayers were washed repeatedly to remove non-adherent PS-NCs-DOX and cells were fixed in 10% formalin (in PBS) and the cell nuclei were stained with 4′,6-diamidino-2-phenylindole (DAPI). Macrophages were observed by CLSM (Olympus IX 81, Center Valley, PA, USA) equipped with a ×60 oil objective lens.

In vitro evaluation against intra-macrophage amastigotes of L. donovani

The J774A.1 macrophage cell line was used for the *in vitro* intracellular drug efficacy test. The macrophages were resuspended at 2.5×10^5 cells/mL in serum-free RPMI-1640. Cell suspensions (200 μL/well) were plated on eight-chamber Lab-Tektissue culture slides (Nunc, USA) and were allowed to adhere for 2 h in a CO_2 incubator with 5% CO_2 at 37°C. The wells were washed twice with serum-free medium, and the adherent macrophages were infected with metacyclic-stage parasites of *L. donovani*, maintaining a *Leishmania*:macrophage ratio of 10:1 in a 200 μL final solution of a complete medium, and incubated overnight. After 24 h, free promastigotes were washed with serum-free medium and infected macrophages were incubated with medium containing free doxorubicin, NCs-DOX and PS-NCs-DOX for 48 h at 37°C at various concentrations. Untreated infected macrophages served as control. The slides were fixed with methanol and stained with Giemsa. At least 100 macrophage nuclei were counted per well for calculating the percentage of infected macrophages and the number of amastigotes per 100 macrophages. Percentage parasite inhibition in treated wells was calculated using the formula $100-(T\times100/C)$,[25] where T is the number of parasites in treated samples/100 macrophage nuclei, and C is the number of parasites in the control. The IC_{50} (concentration of drug that inhibits 50% of *L. donovani* amastigotes) was obtained by plotting a graph of the percentage of inhibition at different concentrations of the formulations using Origin 6.1 version software, and was expressed in ng/mL.

Cytotoxicity studies

The *in vitro* cytotoxicity of blank formulations was measured with the MTT proliferation assay.[26] The experiments were carried out on cells in the exponential growth phase. J774A.1 and RAW macrophage cells were seeded into 24-well plates at 5×10^4 cells/well and were allowed to adhere overnight. The growth medium was replaced with fresh medium and then cells were incubated for 24 h with different blank formulations (NCs and PS-NCs). Cells were then washed twice with 1 mL of PBS. Cells were then incubated in a growth medium containing 1 mg/mL of MTT for 4 h at 37°C, and then 500 μL of DMSO was added to each well to ensure solubilization of the formazan crystals. The optical density was measured using a multi-well scanning spectrophotometer (MRX Microplate Reader, Dynatech Laboratories Inc., Chantilly, VA, USA) at a wavelength of 570 nm.

Animal host

Laboratory-bred male Syrian golden hamsters (*Mesocricetus auratus*, 45–50 g, for *in vivo* antileishmanial activity) and Wistar rats (150–200 g, for pharmacokinetic analysis) from the animal house facility of the Central Drug Research Institute (CDRI) were used as the experimental host after approval from the Institutional Animals Ethical Committee (IAEC) of CDRI (IAEC approval number 70/11/Pharmaceutics/IAEC). The study was carried out under the guidelines of the Council for the Purpose of Control and Supervision of Experiments on Animals (CPCSEA), Ministry of Social Justice and Empowerment, Government of India.

Plasma and tissue sample analysis

Wistar rats weighing ∼150–200 g were divided into three groups of three rats each. Free doxorubicin, NCs-DOX and PS-NCs-DOX containing equivalent doses of doxorubicin (5 mg/kg of body weight) were administered intravenously to different groups. Animals from each group were sacrificed 0.5, 1, 2, 4, 8, 12 and 24 h after administration of the formulations. Blood samples were collected by cardiac puncture. The liver and spleen of the dissected rats were excised, isolated, washed with distilled water and blot dried using tissue paper.[27] Doxorubicin was extracted from 200 μL of each plasma and tissue sample (liver and spleen, 100 mg homogenized in 1 mL of phosphate buffer) using 250 μL of a 50:50 (v/v) mixture of methanol and 40% $ZnSO_4$.[28] After 5 min of vigorous stirring followed by centrifugation, the organic phases were collected and evaporated to dryness at 30°C under a flow of nitrogen. Dry residues from plasma and tissues were dissolved in 100 μL of mobile phase and 50 μL of the resulting solution was injected into the chromatograph.

The samples were analysed by reverse-phase HPLC as reported previously with slight modification.[22] In brief, the HPLC system (CLASS-VP, Shimadzu Corporation, Kyoto, Japan) consisted of a binary gradient pump (LC-20AT), fluorescence detector (RF-10AxL) and system controller (SCL-10A). The CLASS-VP workstation was used for data acquisition. The analytical C18 column (LiChrospher, 5 μm, 250×4 mm) was used for the chromatographic separation of doxorubicin. The mobile phase consisted of a mixture of acetonitrile and water (35/65, v/v) with the pH adjusted to 2.05 using orthophosphoric acid, and detection was carried out at an excitation and emission wavelength of 480 and 550 nm, respectively, at a flow rate of 1 mL/min. The recovery of doxorubicin was determined by comparing the responses of the pre-extracted standard versus responses of post-extracted plasma and tissue standards at equivalent concentration.

In vivo antileishmanial activity

Parasites

Promastigotes of the WHO reference strain, *L. donovani* (M HO-M/IN/80/Dd8), were cultured in RPMI-1640 medium (Sigma-Aldrich, USA) supplemented with 10% FBS (Sigma-Aldrich, USA), penicillin (100 U/mL) and

streptomycin (100 mg/mL) at 26°C. Parasites were also maintained through *in vivo* serial passages (amastigote to amastigote) in hamsters.[29,30]

Antileishmanial activity testing

The isolation of parasites and infection of naive hamsters were carried out as described previously.[31] Briefly, infected animals with a 40–60-day-old infection were autopsied and the spleen was removed aseptically, homogenized in PBS and centrifuged at 900 rpm for 5 min at 4°C to sieve out tissue debris. Supernatant was centrifuged at 3500 rpm for 10 min. The pellet was washed twice with PBS and resuspended to obtain a concentration of 1×10^7 amastigotes per 100 μL of PBS and this inoculum was injected into each hamster intracardially. After 25 days, infection was confirmed by Giemsa staining of tissue smears of spleen after the biopsy of two animals. Infected animals harbouring 38–40 amastigotes/100 macrophage nuclei were then distributed for drug treatment in the following manner: (i) infected controls (no therapy was given); (ii) free doxorubicin; (iii) NCs-DOX; (iv) PS-NCs-DOX; (v) blank NCs; and (vi) blank PS-NCs.

Infected hamsters were treated intraperitoneally with 250 μg/kg/day of doxorubicin in all formulations for four consecutive days. After 15 days post-treatment, splenic biopsies were performed and the parasite burden was determined by counting the number of amastigotes.[32]

Measurement of haemolysis

The degree of haemolysis induced by NCs and PS-NCs on fresh citrated human blood was determined.[33] Red blood cells (RBCs) were obtained from male Wistar rats by centrifugation (1500 rpm, 10 min), washed three times with isotonic 120 mM phosphate sodium chloride buffer (pH 7.4) and suspended in the same buffer at a concentration equivalent to 5% of the normal haematocrit; 40 μL aliquots of this RBC suspension were added to 1 mL of NCs and PS-NCs, incubated at 37°C for 2 h and then centrifuged at 10000 rpm for 20 min. The haemoglobin released in the supernatant was measured spectrophotometrically at 550 nm. The absorbance (A) at this wavelength was directly proportional to the haemoglobin concentration, which was in turn proportional to the number of intact RBCs that were not destroyed by the added sample. For the control, blood was similarly incubated with 0.9% (w/v) saline. Haemolysis induced with hypertonic saline (A2) was taken as 100%. The amount of haemoglobin released into the supernatant by the sample was recorded as A1 and the percentage of haemolysis was calculated as $A2-A1/A2\times100$.

Statistical analysis

All results are given as means ± SD ($n=3$). Differences between formulations were compared using one-way analysis of variance (ANOVA) followed by the Tukey–Kramer multiple comparison test, using InStat software (GraphPad Software Inc., CA, USA). $P<0.05$ denotes significance in all cases.

Results

Preparation of NCs

The low-energy emulsification method was used to prepare nanoemulsion cores and to deposit additional polyelectrolytes on the surface to form a three-layered shell. This procedure represents an innovative and preferable means for the production of polyelectrolyte NCs. In the first step, a nanoemulsion core (oil in water) was obtained from a mixture of SBO (20 wt%) and a ratio of surfactants (Span 80/Tween 80) of ~0.43/0.57 by gradual addition of the aqueous phase containing PSS at the rate of 1 mL/min with gentle agitation using a magnetic stirrer. The temperature of the mixture was maintained at 60°C. In the second step, sequential addition of PRM and SA to nanoemulsion cores led to the formation of polyelectrolyte NCs in LBL fashion. The rigidity of the shell and the zeta-potential were also found to be altered at each layering of PRM and SA. Figure 1(a and b) shows the morphological characteristics of the nanoemulsion core and polyelectrolyte NCs by TEM. Polyelectrolyte layering was observed as a continuous opaque layer (Figure 1)(b) over a nanoemulsion core (Figure 1)(a).

Entrapment efficiency in NCs was found to be 81.37% ± 3.76%. The PS coating on NCs did not significantly affect entrapment efficiency. The nanoemulsion core was negatively charged, initially with a zeta-potential of (−)34.12 ± 2.41 mV due to PSS, and mean diameter of 322 ± 4.31 nm [polydispersity index (PDI) 0.13 ± 0.02]. The first PRM layer reversed the charge to (+)42.11 ± 3.22 mV, while the

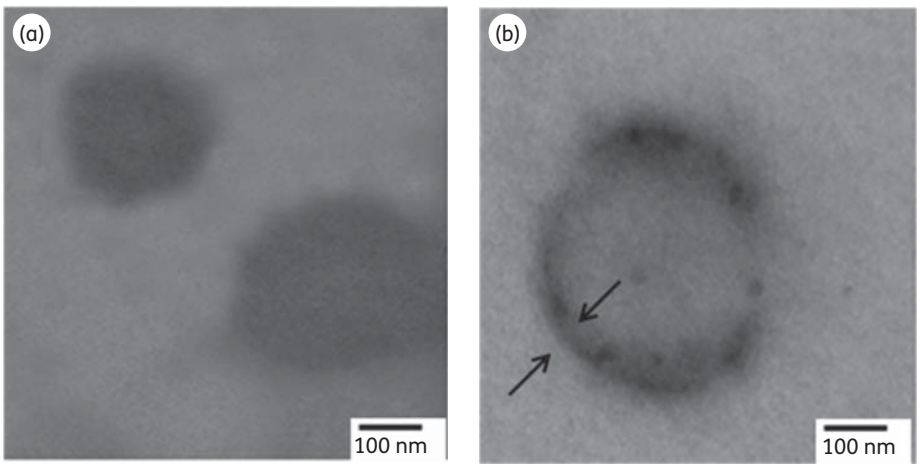

Figure 1. Visualization of nanoemulsion core (a) and polyelectrolyte NCs (b) by TEM. The outer dark layer continuously covering the nanoemulsion core in polyelectrolyte NCs is clearly visible.

Table 1. Characterization of NC and PS-NC formulations

Formulation	Charge (mV)	Size (nm)	Entrapment efficiency (%)
NCs	(+)36.42 ± 2.48	356 ± 2.12	81.37 ± 3.76
PS-NCs	(−)13.23 ± 2.16	371 ± 1.02	80.13 ± 6.43

Values are expressed as means ± SD.

subsequent SA layer reversed the charge to (−)35.64 ± 3.09 mV. The final PRM layer assembled on the SA layer changed the zeta-potential value finally to (+)36.42 ± 2.48 mV. Depending on the type of polyelectrolyte added, the zeta-potential altered at every layering, confirming LBL assembly over the nanoemulsion core. Table 1 shows the particle sizes and size distributions of different formulations measured by differential light scattering. The results indicate that the mean diameter of NCs was 356 ± 2.12 nm (PDI 0.22 ± 0.03).

NCs coated with PS-terminating ligand

The NC formulation was finally coated with PS by hydrating the phospholipid film with an NC dispersion. The concluding PRM layer on the NCs facilitated spreading of PS uniformly over the NCs (Figure S1, available as Supplementary data at *JAC* Online), which was confirmed by a change in the zeta-potential to (−)13.23 ± 2.16 mV. The process variable, i.e. the PS/PRM weight ratio, was optimized by measuring the change in zeta-potential of the dispersion in triple-distilled water at 25°C (Zetasizer 3000 HS; Malvern Instruments Co.) (Figure S2, available as Supplementary data at *JAC* Online). No change in zeta-potential was observed above a PS:PRM weight ratio of 0.05:0.1; this ratio was therefore selected as the optimum for preparing PS-NCs. Additionally, the presence of PS on the surface of NCs was verified by using an FITC-conjugated PS-specific protein, annexin V, by measuring its characteristic fluorescence. After treatment of PS-NCs with FITC-conjugated annexin V, robust fluorescence was visible. To rule out the formation of PS vesicles during coating on NCs, DSC was performed since phase transition is an important characteristic of lipid layers. It is evident from the thermogram (Figure S3, available as Supplementary data at *JAC* Online) that PS assembled on NCs observed a phase transition, which was 10°C below the phase transition of PS vesicles suspended in water. This lower value of phase transition temperature of PS assembled on NCs could be attributed to the disordering effect of polyelectrolyte molecules due to mutual interaction between polyelectrolyte and lipid headgroups. Table 1 shows the particle size and size distributions of NCs and PS-NCs measured by differential light scattering. The results indicate that the mean diameters of NCs and PS-NCs were 356 ± 2.12 nm (PDI 0.22 ± 0.03) and 371 ± 1.02 nm (PDI 0.15 ± 0.03), respectively.

In vitro uptake studies

Figure 2 shows the macrophagic uptake of various NC formulations in the J774A.1 macrophage cell line as shown by flow cytometry. This study represents the comparative uptake of free doxorubicin, NCs-DOX and PS-NCs-DOX. Figure 2 shows almost 3-fold (>2.9) enhanced uptake of NCs-DOX compared with free doxorubicin, while PS-NCs-DOX showed almost 2-fold (>1.75)

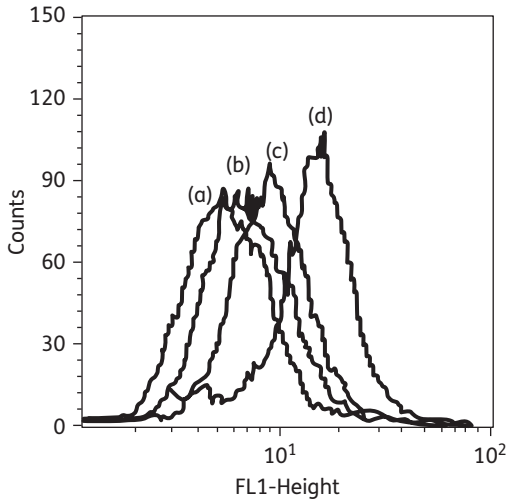

Figure 2. Flow cytometric diagram for uptake studies in macrophagic J774A.1 cells. The *x*-axis represents fluorescence inside the cells. (a) Control cells. (b) Free doxorubicin. (c) NCs-DOX. (d) PS-NCs-DOX.

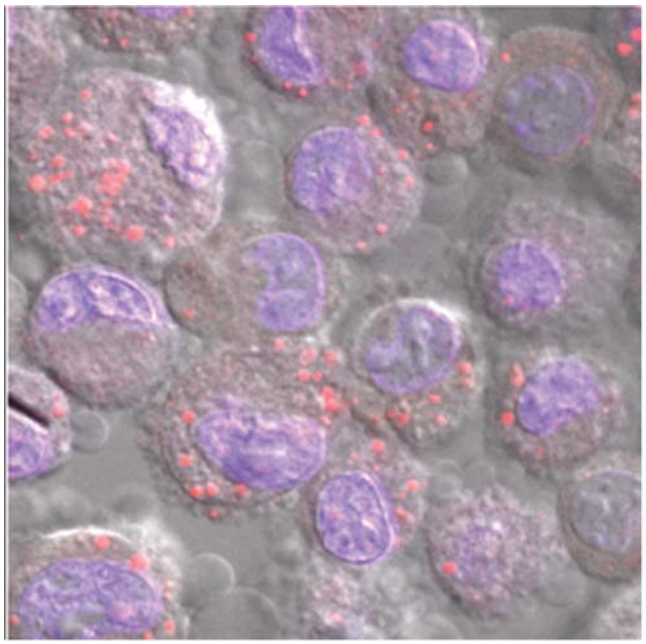

Figure 3. CLSM images of fluorescently labelled adherent cell cultures treated with PS-NCs-DOX. There is complete internalization of PS-NCs-DOX in macrophages (red fluorescent signal arising from doxorubicin and blue fluorescence arising from DAPI, a nucleus-staining dye). This figure appears in colour in the online version of *JAC* and in black and white in the print version of *JAC*.

increased uptake in J774A.1 cell lines compared with NCs. The typical confocal microscopic pictures shown in Figure 3 illustrate the distribution of internalized PS-NCs-DOX within cells. Most of the capsules are internalized within cells, as was manifest from the merged confocal image, showing the co-localization of red fluorescent signal arising from doxorubicin and blue fluorescence arising from DAPI, a nucleus-staining dye (Figure 3).

In vitro evaluation against intra-macrophage amastigotes of L. donovani

Inhibition of amastigote multiplication within macrophages by free doxorubicin, NCs-DOX and PS-NCs-DOX was recorded. All samples were stained and the number of infected macrophages was determined microscopically. Both NCs-DOX and PS-NCs-DOX showed significant improvement ($P<0.01$) in efficacy in comparison with free doxorubicin. Similarly, PS-NCs-DOX showed a significant improvement ($P<0.05$) in efficacy in comparison with NCs-DOX (Table 2).

Pharmacokinetics of doxorubicin formulations in rats

The plasma concentration–time profile of different doxorubicin formulations in rats at a dose of 5 mg/kg is presented in Figure 4. High mean residence time (MRT) and lower clearance was observed in PS-NCs-DOX compared with NCs-DOX and free doxorubicin. The pharmacokinetic parameters of free doxorubicin, NCs-DOX and PS-NCs-DOX are given in Table 3. The extraction recovery of doxorubicin from plasma was 93.47%±2.89%.

Table 2. *In vitro* activity of doxorubicin formulations against *L. donovani* intra-macrophagic amastigotes

			Level of significance		
	Formulation	IC_{50} (ng/mL)	A	B	C
A	free doxorubicin	691.67±10.41	—	$P<0.01$	$P<0.01$
B	NCs-DOX	391.67±20.40		—	$P<0.05$
C	PS-NCs-DOX	354.33±5.13			—

Results are expressed as inhibition of parasite growth (IC_{50}) observed after 48 h of incubation; values are expressed as means±SD ($n=3$).

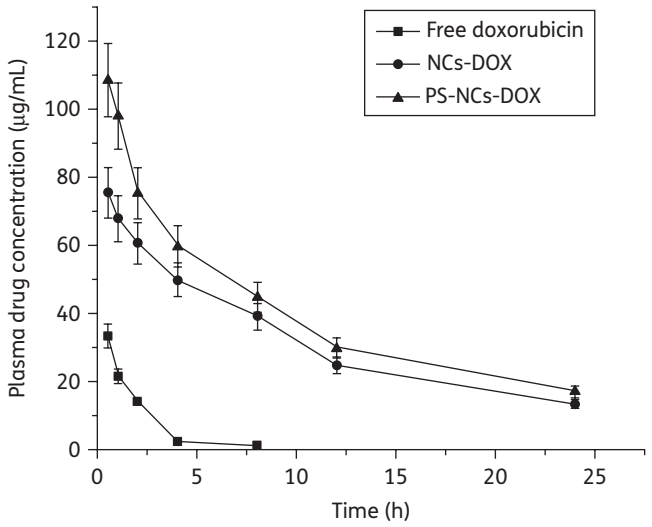

Figure 4. Plasma drug concentration (μg/mL) versus time (h) profile of different doxorubicin formulations administered intravenously at 5 mg/kg of body weight in Wistar rats. Data are presented as means±SD ($n=3$).

Liver and spleen distribution of different doxorubicin formulations

The doxorubicin concentrations in liver and spleen after intravenous injection of different doxorubicin formulations are shown in Figure 5. PS-NCs-DOX and NCs-DOX showed significantly higher localization of doxorubicin at all timepoints compared with free doxorubicin ($P<0.05$). Similarly, PS-NCs-DOX showed enhanced drug distribution compared with NCs-DOX in liver and spleen. The extraction recoveries of doxorubicin from liver and spleen were 91.36%±3.12% and 88.34%±5.38%, respectively.

In vivo antileishmanial activity testing

There was significant improvement in activity with PS-NCs-DOX when compared with NCs-DOX ($P<0.05$). PS-NCs-DOX caused 85.23%±4.49% inhibition of the splenic parasitic burden, whereas NCs-DOX and free doxorubicin caused only 72.88%±3.87% and 42.85%±2.11% parasite inhibition, respectively, in *Leishmania*-infected hamsters ($P<0.01$ for PS-NCs-DOX versus free doxorubicin and NCs-DOX versus free doxorubicin). The parasite inhibition with blank PS-NCs and NCs was found to be 18.73%±2.79% and 13.8%±4.37%, respectively, as shown in Figure 6 ($P<0.05$ for PS-NCs versus NCs).

Cytotoxicity studies

The cytotoxicity of the different formulations was determined by the MTT assay. NCs showed 96% and 94% while PS-NCs showed 94% and 93% cell viability after 6 h of incubation in J774A.1 and RAW macrophagic cell lines, respectively.

Measurement of haemolysis

Blank NCs and PS-NCs showed 6.92%±3.34% and 5.82%±1.71% haemolytic activity, respectively, after 2 h of incubation.

Discussion

Chemotherapy of leishmaniasis primarily consists of the administration of antimonials [sodium stibogluconate (Pentostam) or *N*-methylglucamine antimoniate (Glucantime)], but responses to these drugs are abating due to the emergence of resistance, which causes frequent relapses. Pentamidine and amphotericin B have been the second-line treatment of leishmaniasis after antimony failure; however, their application is greatly limited due to their toxic manifestations.

There is a great requirement for new therapeutics due to the increasing financial burden arising from drug-resistant *Leishmania* strains.[34,35] Doxorubicin, an anthracycline antibiotic used for the chemotherapy of various human cancers, is emerging as a potential antileishmanial agent with acceptable toxicity at limited doses.[4,36] Attempts are therefore being made to develop a novel delivery system with a high payload of chemotherapeutic agent that is affordable and stable and reduces the obstacle of toxicity. Production of NCs by the LBL method has numerous therapeutic benefits, such as readily tailored physical properties (e.g. size, composition, porosity, stability, surface functionality and colloidal stability), high payload efficiency, controlled and targeted release at the site of infection, and

Table 3. Pharmacokinetic parameters following intravenous administration of various formulations of doxorubicin in rats

Formulation	MRT (h)	C_{max} (μg/mL)	Clearance (mL/h/kg)	AUC (h·μg/mL)
Free doxorubicin	1.41 ± 0.29	33.16 ± 4.43	13.14 ± 1.24	74.55 ± 3.14
NCs-DOX	8.13 ± 0.13	75.26 ± 3.10	1.03 ± 0.03	779.24 ± 9.81*
PS-NCs-DOX	9.03 ± 3.14	108.37 ± 2.55	0.60 ± 0.04	1056.70 ± 4.74*,**

Values are expressed as means ± SD.
Significance versus free doxorubicin: *$P < 0.01$.
Significance for PS-NCs-DOX versus NCs-DOX: **$P < 0.01$.

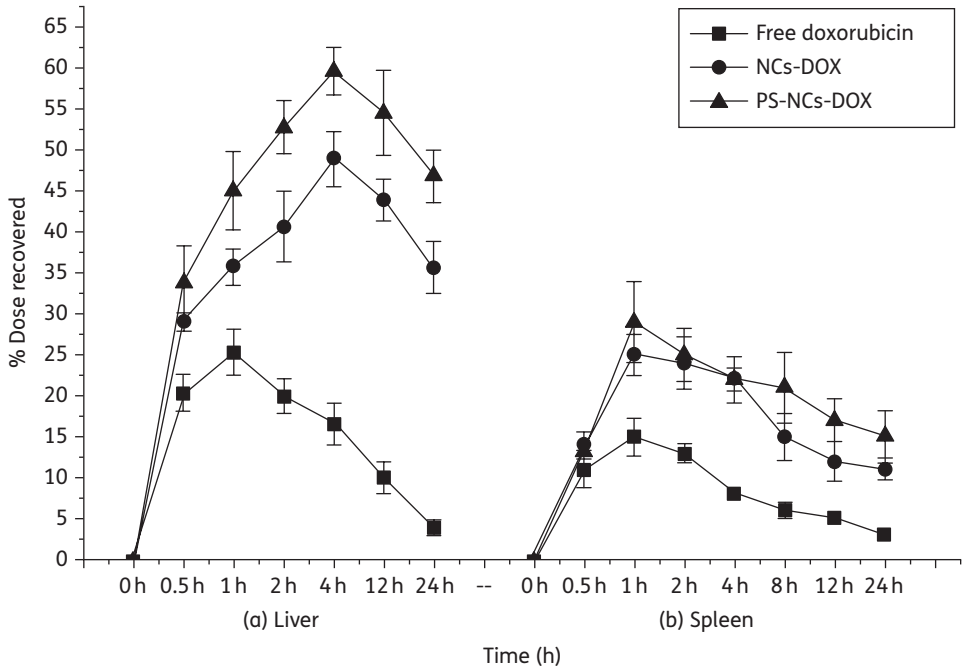

Figure 5. Percentage of dose recovered for different doxorubicin formulations in liver (a) and spleen (b). Data show the effect of NCs-DOX and PS-NCs-DOX on hepatic and splenic uptake of doxorubicin. PS-NCs-DOX show significantly enhanced uptake in comparison with NCs-DOX ($P < 0.05$).

increased stability, solubility and pharmacokinetic profile, over other nanoarchitectures.[37–40] Apart from this, there is the possibility of numerous therapeutic benefits over liposomes, such as resistance to physiological stress and the possibility of oral delivery.[41]

There are several reports of the use of inorganic core particles to fabricate LBL-based capsules.[42,43] It has been observed by our group that preparing inorganic core particles, i.e. $CaCO_3$ and $Ca(PO_4)_2$, leads to the formation of several polymorphs,[44] which hampers the formation of uniform layering of polyelectrolytes over the core. Similarly, the particle size of the core particle remains in the range of 3–5 μm, which may not be suitable for various applications. In the present investigation, we used a nanoemulsion with a core particle size range of 200–300 nm.

We used a nanoemulsion core for fabrication of NCs, in which doxorubicin was encapsulated with a high payload due to physicochemical properties. The nanoemulsion was chosen as a core with a view to improving the loading efficiency of doxorubicin, since free doxorubicin base has higher affinity for the internal oil phase and this restricts its entry into the external aqueous phase.

We used SA and PRM for the preparation of polyelectrolyte NCs. Both these polyelectrolytes are biocompatible and biodegradable. Drug incorporation in nanoparticles of biocompatible polymers has an advantage over other systems due to ease of preparation, longer shelf life and greater stability in biological fluids without any adverse effects. However, to prepare polyelectrolyte-based NCs in LBL fashion, the core particle must have some initial charge. We therefore incorporated PSS due to its surface adsorbing properties along with its ability to impart a highly negative charge to the nanoemulsion core. This initial negative charge facilitates the deposition of cationic PRM as a first layer. Subsequently, oppositely charged SA and PRM were used to develop NCs. The method of complex coacervation was used to form a capsule shell consisting of PRM-SA-PRM layers interlinked as a polyelectrolyte complex. The alternate coating of PRM and SA over the nanoemulsion core was confirmed by reversal of the zeta-potential at each layering. TEM images show

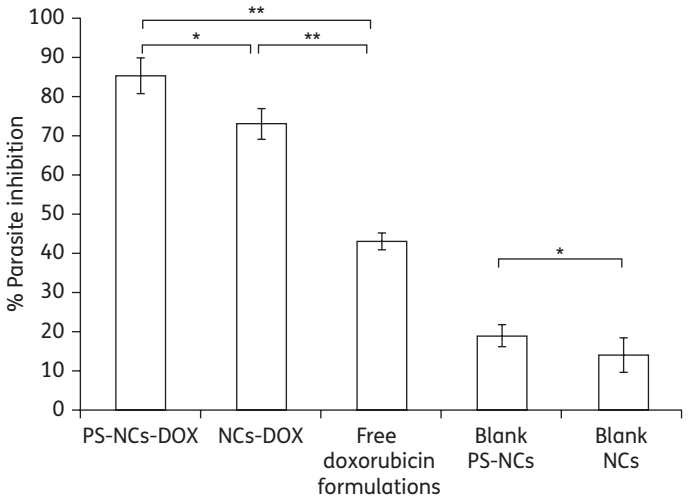

Figure 6. Antileishmanial activity of doxorubicin formulations against established infection of *L. donovani* in hamsters. Drug formulations (equivalent to 250 μg/kg/day for 4 consecutive days) and formulations without drug were injected intraperitoneally into each hamster on day 31 post-infection. The parasite burden was estimated by splenic biopsy on day 15 post-treatment and percentage parasite inhibition was calculated in comparison with the parasite burden of untreated infected animals (means ± SD) ($n=3$). The mean parasite burden in the spleen of untreated, infected control animals was 413 ± 45.90 amastigotes per 100 cell nuclei of macrophages. *$P<0.05$ (comparison of PS-NCs-DOX versus NCs-DOX and blank PS-NCs versus NCs), **$P<0.01$ (comparison of PS-NCs-DOX versus free doxorubicin and NCs-DOX versus free doxorubicin).

that there was an opaque layer of polyelectrolytes (Figure 1)(b) over a plain nanoemulsion core (Figure 1)(a). Due to the presence of PRM as an outermost layer, the NCs had a net positive charge on the surface. The phospholipid PS has a net negative charge, which is the driving force for its adsorption over positively charged NCs (Figure S1). However, it has been reported that if oppositely charged vesicles are formed in the presence of charged polyelectrolytes, they adhere over the polyelectrolyte surface and subsequently spread as a uniform layer on incubation.[21,45] Furthermore, the DSC chromatogram showed a 10°C difference in the phase transition temperature of PS vesicles and PS-coated NCs. This difference in phase transition temperature might be attributed to the formation of a uniform layer of PS on the surface of NCs, which rules out the formation of PS vesicles (Figure S3). The phospholipid readily adsorbs on the PRM as a result of specific interaction of amino groups of PRM with carboxyl and phosphate groups of the phospholipid.[21,45] Due to the adsorption of PS on NCs, the surface charge changes to negative and approaches a minimum value at a PS:PRM weight ratio of 0.05:0.1 (Figure S2). This negative zeta-potential indicates that a positive charge has been camouflaged by PS. On further addition of PS (beyond a PS:PRM weight ratio of 0.05:0.1) there was no further change in zeta-potential, which may be attributed to saturation of the PRM layer due to PS. The coating of PS on the surface of NCs was confirmed by using an FITC-conjugated PS-specific protein, annexin V, by measuring its characteristic fluorescence. When PS-NCs were treated with FITC-conjugated annexin V, characteristic fluorescence was evident, indicating the presence of PS on the surface of NCs. It has been reported that annexin V specifically binds to PS.[46] A flow cytometry study revealed almost doubled (>1.75) uptake in J774A.1 macrophage cells by PS-NCs-DOX compared with NCs-DOX (Figure 2). The higher uptake of PS-NCs-DOX was confirmed by a CLSM study showing complete internalization of PS-NCs-DOX in macrophages (Figure 3). This significantly higher efficacy of PS-NCs-DOX *in vitro* ($P<0.05$) compared with NCs-DOX (Table 2) may be attributed to the facilitated uptake of NCs due to the presence of the specific ligand PS. It has been reported that macrophages have multiple receptors for the recognition of PS, which results in prolonged residence of doxorubicin inside macrophages.[8]

This higher uptake of PS-NCs-DOX compared with NCs-DOX in macrophages is of interest in the sense that there is scope for the enhanced localization of these modified NCs by intramacrophage amastigotes in liver and spleen, which may be significant for visceral leishmaniasis. Pharmacokinetic parameters showed that the AUC of PS-NCs-DOX was increased 14.17- and 1.35-fold, while the MRT was increased 6.39- and 1.11-fold compared with free doxorubicin and NCs-DOX, respectively, with a corresponding decrease in clearance. Similarly, significantly higher MRT and lower clearance with PS-NCs-DOX indicates efficient macrophage targeting compared with NCs-DOX. The MRT of NCs-DOX and PS-NCs-DOX was found to be 8.13 ± 0.13 and 9.03 ± 3.14 h, respectively. The complex pharmacokinetics of PS-NCs-DOX might be attributed to its restricted distribution in the body due to the presence of the highly specific ligand PS on the surface of NCs.[47] In our experimental conditions it seems there is non-linear clearance with saturation of the reticuloendothelial system, such as the liver and spleen, and redistribution of doxorubicin into the circulation. The data are consistent with the non-linear saturation-like kinetic profile, resulting in sustained plasma levels and decreased clearance. Apart from this, higher unspecific serum protein binding of the PS-NCs-DOX may also be responsible for its lower clearance. This complex pharmacokinetics may improve pharmacotherapy using doxorubicin due to reduction of possible adverse events because encapsulated doxorubicin will not be available directly to the other body tissues. Greater localization of doxorubicin by PS-NCs-DOX compared with NCs-DOX in both the liver and the spleen confirmed that most of the drug was rapidly localized in the liver and spleen due to enhanced uptake by macrophages (Figure 5).

Several receptors are involved in the recognition of PS, including some that can recognize naked PS and function together with additional receptors that bind bridging protein-bound PS.[8] There are bridging molecules, termed GAS6 and Protein S, that can bind PS and in turn be recognized by engulfment receptors expressed by phagocytes.[48,49] Similarly, there is another soluble bridging molecule, termed MFGE8 (milk fat globule EGF factor 8 protein), secreted by macrophages, which then engulf MFGE8-coated apoptotic cells (PS is exposed on the outer leaflet of the cells) through $\alpha_v\beta_3$-integrin.[50] There is also another membrane protein expressed by macrophages, namely Bal1 (brain angiogenesis inhibitor 1), that can directly recognize PS exposed on apoptotic cells.[51] Several receptors have been suggested to play a pivotal role in mediating PS recognition, including scavenger receptors (class B, CD36/SR-BI; and class A, MARCO),[52] CD68 (an oxLDL receptor), CD14, annexins, β2

glycoprotein I and GAS6.[9] Tempone *et al*.[53] described the macrophage-targeting ability of PS liposomes towards scavenger receptors and developed drug-loaded PS liposomes that were found to accumulate to a greater degree in macrophages compared with the free drug.

Macrophagic uptake of PS appended to NCs opens a new area for targeting drug-loaded carrier systems, which was confirmed by the significantly improved *in vivo* antileishmanial activity of PS-NCs-DOX when compared with NCs-DOX ($P<0.05$). Our data show that PS-NCs could be a useful carrier for targeting antileishmanial drugs into macrophages, and, interestingly, PS-NCs also show antileishmanial activity by themselves. Since PS-anchored NCs act as a signal for engulfment by phagocytes, they are specifically recognized by macrophages and are phagocytosed, which subsequently leads to macrophage activation. There are several reports that demonstrate that macrophage activation leads to rapid parasite killing and digestion.[54] It has also been reported that up-regulation of inducible nitric oxide synthase (iNOS) and subsequent nitric oxide (NO) production are important for the parasiticidal activity of infected macrophages during experimental infection.[54,55] The polyelectrolytes PRM and SA have been shown to induce the iNOS pathway, which results in subsequent production of NO.[56,57]

The primary objective of our work was to employ the naturally occurring 'eat me' signal, PS, as a specific ligand that is recognized by phagocytes. The superior efficacy of the encapsulated doxorubicin in eliminating intracellular amastigotes of *L. donovani* in both an *in vitro* macrophage model and an *in vivo* hamster model of visceral leishmaniasis demonstrates the effectiveness of this approach. Results clearly indicate a substantial enhancement of the efficacy of PS-NCs-DOX compared with NCs-DOX due to anchoring of PS.

To evaluate the safety profile of formulations on cells, a cell viability study was carried out in J774A.1 and RAW macrophage cells. The almost negligible cytotoxicity of both NCs and PS-NCs in J774A.1 and RAW macrophagic cells confirms that these excipients are safe to use. To evaluate the safety profile of the developed formulation, the haemolytic activity was measured with different NC formulations. Haemolysis was <6% when tested with both formulations, suggesting no deleterious effects on erythrocytes.

Conclusions

The present investigation provides evidence that the prototype formulation may be used for efficient treatment of leishmaniasis via PS-specific ligand-anchored NCs bearing doxorubicin. We report that PS-NCs provide an 'eat me' signal for specialized phagocytes because recognition of PS involves multiple receptors present on the phagocyte and causes enhanced internalization of the bioactive molecule into cells. Enhanced uptake directly reduces the dosage of the formulation, which is highly desirable for optimizing the therapeutic effect and reducing the side effects of doxorubicin.

Acknowledgements

P. R. M. is grateful to the Indian Council of Medical Research, New Delhi, India, for providing financial support. S. K. is grateful to the Indian Council of Medical Research, New Delhi, India, for providing SRF fellowships. The authors are particularly grateful to Mr Vishwakarma, SAIF, CDRI, Lucknow, for the flow cytometry study. This is CDRI Communication No. 8275.

Funding

This work was supported by a grant from the Indian Council of Medical Research, New Delhi, India (GAP 0085).

Transparency declarations

None to declare.

Supplementary data

Figures S1–S3 are available as Supplementary data at *JAC* Online (http://jac.oxfordjournals.org/).

References

1 Trotter ER, Peters W, Robinson BL. The experimental chemotherapy of leishmaniasis, IV. The development of a rodent model for visceral infection. *Ann Trop Med Parasitol* 1980; **74**: 127–38.

2 Badaró R, Jones TC, Lorenço R *et al*. A prospective study of visceral leishmaniasis in an endemic area of Brazil. *J Infect Dis* 1986; **154**: 639–49.

3 Chono S, Tanino T, Seki T *et al*. Efficient drug targeting to rat alveolar macrophages by pulmonary administration of ciprofloxacin incorporated into mannosylated liposomes for treatment of respiratory intracellular parasitic infections. *J Control Release* 2008; **127**: 50–8.

4 Kole L, Das L, Das PK. Synergistic effect of interferon-γ and mannosylated liposome-incorporated doxorubicin in the therapy of experimental visceral leishmaniasis. *J Infect Dis* 1999; **180**: 811–20.

5 Kelly C, Jefferies C, Cryan SA. Targeted liposomal drug delivery to monocytes and macrophages. *J Drug Deliv* 2011; **2011**: 727241.

6 Ravichandran KS, Lorenz U. Engulfment of apoptotic cells: signals for a good meal. *Nat Rev Immunol* 2007; **7**: 964–74.

7 Fadok V, Voelker D, Campbell P *et al*. Exposure of phosphatidylserine on the surface of apoptotic lymphocytes triggers specific recognition and removal by macrophages. *J Immunol* 1992; **148**: 2207–16.

8 Wu Y, Tibrewal N, Birge RB. Phosphatidylserine recognition by phagocytes: a view to a kill. *Trends Cell Biol* 2006; **16**: 189–97.

9 Fadok V, Bratton D, Frasch S *et al*. The role of phosphatidylserine in recognition of apoptotic cells by phagocytes. *Cell Death Differ* 1998; **5**: 551–62.

10 Mietto L, Boarato E, Toffano G *et al*. Internalization of phosphatidylserine by adherent and non-adherent rat mononuclear cells. *Biochim Biophys Acta* 1989; **1013**: 1–6.

11 Fidler IJ, Raz A, Fogler WE *et al*. Design of liposomes to improve delivery of macrophage-augmenting agents to alveolar macrophages. *Cancer Res* 1980; **40**: 4460–6.

12 Sundar S, Rai M. Advances in the treatment of leishmaniasis. *Curr Opin Infect Dis* 2002; **15**: 593–8.

13 Gille L, Nohl H. Analyses of the molecular mechanism of adriamycin-induced cardiotoxicity. *Free Radic Biol Med* 1997; **23**: 775–82.

14 Sett R, Basu N, Ghosh AK *et al*. Potential of doxorubicin as an antileishmanial agent. *J Parasitol* 1992; **78**: 350–4.

15 Sanchez-Brunete JA, Dea MA, Rama S *et al*. Treatment of experimental visceral leishmaniasis with amphotericin B in stable albumin microspheres. *Antimicrob Agents Chemother* 2004; **48**: 3246–52.

16 Tardi P, Boman N, Cullis P. Liposomal doxorubicin. *J Drug Target* 1996; **4**: 129–40.

17 Gupta GK, Kansal S, Misra P *et al*. Uptake of biodegradable gel-assisted LBL nanomatrix by *Leishmania donovani*-infected macrophages. *AAPS PharmSciTech* 2009; **10**: 1343–7.

18 Tewes F, Munnier E, Antoon B *et al*. Comparative study of doxorubicin-loaded poly(lactide-co-glycolide) nanoparticles prepared by single and double emulsion methods. *Eur J Pharm Biopharm* 2007; **66**: 488–92.

19 Liu W, Sun D, Li C *et al*. Formation and stability of paraffin oil-in-water nano-emulsions prepared by the emulsion inversion point method. *J Colloid Interface Sci* 2006; **303**: 557–63.

20 Kataoka K, Matsumoto T, Yokoyama M *et al*. Doxorubicin-loaded poly(ethylene glycol)–poly(β-benzyl-l-aspartate) copolymer micelles: their pharmaceutical characteristics and biological significance. *J Control Release* 2000; **64**: 143–53.

21 Moya S, Donath E, Sukhorukov GB *et al*. Lipid coating on polyelectrolyte surface modified colloidal particles and polyelectrolyte capsules. *Macromolecules* 2000; **33**: 4538–44.

22 Hartmann G, Vassileva V, Piquette-Miller M. Impact of endotoxin-induced changes in P-glycoprotein expression on disposition of doxorubicin in mice. *Drug Metab Dispos* 2005; **33**: 820–8.

23 Duverger A, Jackson RJ, van Ginkel FW *et al*. *Bacillus anthracis* edema toxin acts as an adjuvant for mucosal immune responses to nasally administered vaccine antigens. *J Immunol* 2006; **176**: 1776–83.

24 Albright CF, Graciani N, Han W *et al*. Matrix metalloproteinase-activated doxorubicin prodrugs inhibit HT1080 xenograft growth better than doxorubicin with less toxicity. *Mol Cancer Ther* 2005; **4**: 751–60.

25 Pal R, Anuradha, Rizvi SY *et al*. *Leishmania donovani* in hamsters: stimulation of non-specific resistance by some novel glycopeptides and impact on therapeutic efficacy. *Experientia* 1991; **47**: 486–90.

26 Seymour AA, Sheldon JH, Smith PL *et al*. Potentiation of the renal responses to bradykinin by inhibition of neutral endopeptidase 3.4.24.11 and angiotensin-converting enzyme in anesthetized dogs. *J Pharmacol Exp Ther* 1994; **269**: 263–70.

27 Fundarò A, Cavalli R, Bargoni A *et al*. Non-stealth and stealth solid lipid nanoparticles (SLN) carrying doxorubicin: pharmacokinetics and tissue distribution after i.v. administration to rats. *Pharmacol Res* 2000; **42**: 337–43.

28 Álvarez-Cedrón L, Sayalero ML, Lanao JM. High-performance liquid chromatographic validated assay of doxorubicin in rat plasma and tissues. *J Chromatogr B Biomed Sci Appl* 1999; **721**: 271–8.

29 Dube A, Sharma P, Srivastava JK *et al*. Vaccination of langur monkeys (*Presbytis entellus*) against *Leishmania donovani* with autoclaved *L. major* plus BCG. *Parasitology* 1998; **116**: 219–21.

30 Dube A, Srivastava JK, Sharma P *et al*. *Leishmania donovani*: cellular and humoral immune responses in Indian langur monkeys, *Presbytis entellus*. *Acta Trop* 1999; **73**: 37–48.

31 Dube A, Singh N, Sundar S *et al*. Refractoriness to the treatment of sodium stibogluconate in Indian kala-azar field isolates persist in in vitro and in vivo experimental models. *Parasitol Res* 2005; **96**: 216–23.

32 Guru PY, Agrawal AK, Singha UK *et al*. Drug targeting in *Leishmania donovani* infections using tuftsin-bearing liposomes as drug vehicles. *FEBS Lett* 1989; **245**: 204–8.

33 Wang J-J, Sung KC, Hu OY-P *et al*. Submicron lipid emulsion as a drug delivery system for nalbuphine and its prodrugs. *J Control Release* 2006; **115**: 140–9.

34 Tiuman TS, Santos AO, Ueda-Nakamura T *et al*. Recent advances in leishmaniasis treatment. *Int J Infect Dis* 2011; **15**: e525–e32.

35 Romero EL, Morilla MJ. Drug delivery systems against leishmaniasis? Still an open question. *Expert Opin Drug Deliv* 2008; **5**: 805–23.

36 Shukla A, Patra S, Dubey V. Evaluation of selected antitumor agents as subversive substrate and potential inhibitor of trypanothione reductase: an alternative approach for chemotherapy of leishmaniasis. *Mol Cell Biochem* 2011; **352**: 261–70.

37 Shukla P, Gupta G, Singodia D *et al*. Emerging trend in nano-engineered polyelectrolyte-based surrogate carriers for delivery of bioactives. *Expert Opin Drug Deliv* 2010; **7**: 993–1011.

38 Decher G. Fuzzy nanoassemblies: toward layered polymeric multicomposites. *Science* 1997; **277**: 1232–7.

39 Decher G, Eckle M, Schmitt J *et al*. Layer-by-layer assembled multicomposite films. *Curr Opin Colloid Interface Sci* 1998; **3**: 32–9.

40 Dubas ST, Schlenoff JB. Factors controlling the growth of polyelectrolyte multilayers. *Macromolecules* 1999; **32**: 8153–60.

41 Date AA, Joshi MD, Patravale VB. Parasitic diseases: liposomes and polymeric nanoparticles versus lipid nanoparticles. *Adv Drug Deliv Rev* 2007; **59**: 505–21.

42 Sukhorukov GB, Donath E, Davis S *et al*. Stepwise polyelectrolyte assembly on particle surfaces: a novel approach to colloid design. *Polym Adv Technol* 1998; **9**: 759–67.

43 Volodkin DV, Petrov AI, Prevot M *et al*. Matrix polyelectrolyte microcapsules: new system for macromolecule encapsulation. *Langmuir* 2004; **20**: 3398–406.

44 Vdović N, Kralj D. Electrokinetic properties of spontaneously precipitated calcium carbonate polymorphs: the influence of organic substances. *Colloids Surf E Physicochem Eng Asp* 2000; **161**: 499–505.

45 Romero G, Estrela-Lopis I, Castro-Hartmann P *et al*. Stepwise surface tailoring of carbon nanotubes with polyelectrolyte brushes and lipid layers to control their intracellular distribution and 'in vitro' toxicity. *Soft Matter* 2011; **7**: 6883–90.

46 Vermes I, Haanen C, Steffens-Nakken H *et al*. A novel assay for apoptosis flow cytometric detection of phosphatidylserine expression on early apoptotic cells using fluorescein labelled annexin V. *J Immunol Methods* 1995; **184**: 39–51.

47 Khan MA, Owais M. Toxicity, stability and pharmacokinetics of amphotericin B in immunomodulator tuftsin-bearing liposomes in a murine model. *J Antimicrob Chemother* 2006; **58**: 125–32.

48 Nagata K, Ohashi K, Nakano T *et al*. Identification of the product of growth arrest-specific gene 6 as a common ligand for Axl, Sky, and Mer receptor tyrosine kinases. *J Biol Chem* 1996; **271**: 30022–7.

49 Anderson HA, Maylock CA, Williams JA *et al*. Serum-derived protein S binds to phosphatidylserine and stimulates the phagocytosis of apoptotic cells. *Nat Immunol* 2003; **4**: 87–91.

50 Hanayama R, Tanaka M, Miwa K *et al*. Identification of a factor that links apoptotic cells to phagocytes. *Nature* 2002; **417**: 182–7.

51 Park D, Tosello-Trampont A-C, Elliott MR *et al*. BAI1 is an engulfment receptor for apoptotic cells upstream of the ELMO/Dock180/Rac module. *Nature* 2007; **450**: 430–4.

52 Rigotti A, Acton SL, Krieger M. The class B scavenger receptors SR-BI and CD36 are receptors for anionic phospholipids. *J Biol Chem* 1995; **270**: 16221–4.

53 Tempone AG, Perez D, Rath S *et al*. Targeting *Leishmania* (*L.*) *chagasi* amastigotes through macrophage scavenger receptors: the use of drugs entrapped in liposomes containing phosphatidylserine. *J Antimicrob Chemother* 2004; **54**: 60–8.

54 Nacy CA, Meltzer MS, Fortier AH. Macrophage activation to kill *Leishmania tropica*: characterization of P/J mouse macrophage defects for lymphokine-induced antimicrobial activities against *Leishmania tropica* amastigotes. *J Immunol* 1984; **133**: 3344–50.

55 Mukbel RM, Patten C, Gibson K *et al*. Macrophage killing of *Leishmania amazonensis* amastigotes requires both nitric oxide and superoxide. *Am J Trop Med Hyg* 2007; **76**: 669–75.

56 Takakura K, Mizogami M, Fukuda S. Protamine sulfate causes endothelium-independent vasorelaxation via inducible nitric oxide synthase pathway. *Can J Anaesth* 2006; **53**: 162–7.

57 Son EH, Moon EY, Rhee DK *et al*. Stimulation of various functions in murine peritoneal macrophages by high mannuronic acid-containing alginate (HMA) exposure in vivo. *Int Immunopharmacol* 2001; **1**: 147–54.